AFRL-RX-WP-TP-2012-0377

KINETICS OF PASSIVE OXIDATION OF HI-NICALON-S SiC FIBERS IN WET AIR: RELATIONSHIPS BETWEEN Si02 SCALE THICKNESS, CRYSTALLIZATION, AND FIBER STRENGTH (PREPRINT)

Randall S. Hay and G.E. Fair
Composites Branch
Structural Materials Division

A. Hart and S. Potticary
University of Cincinnati

R. Bouffioux
New Mexico Tech University

JULY 2012
Interim

AIR FORCE RESEARCH LABORATORY
MATERIALS AND MANUFACTURING DIRECTORATE
WRIGHT-PATTERSON AIR FORCE BASE, OH 45433-7750
AIR FORCE MATERIEL COMMAND
UNITED STATES AIR FORCE

REPORT DOCUMENTATION PAGE

Form Approved
OMB No. 0704-0188

1. REPORT DATE *(DD-MM-YY)*	2. REPORT TYPE	3. DATES COVERED *(From - To)*
July 2012	Technical Paper	1 June 2012 – 1 July 2012

4. TITLE AND SUBTITLE
KINETICS OF PASSIVE OXIDATION OF HI-NICALON-S SiC FIBERS IN WET AIR: RELATIONSHIPS BETWEEN Si02 SCALE THICKNESS, CRYSTALLIZATION, AND FIBER STRENGTH (PREPRINT)

5a. CONTRACT NUMBER
In-house

5b. GRANT NUMBER

5c. PROGRAM ELEMENT NUMBER
62102F

6. AUTHOR(S)
Randall S. Hay and G.E. Fair (AFRL/RXCC)
A. Hart and S. Potticary (University of Cincinnati)
R. Bouffioux (New Mexico Tech University)

5d. PROJECT NUMBER
4347

5e. TASK NUMBER
50

5f. WORK UNIT NUMBER
LN102102

7. PERFORMING ORGANIZATION NAME(S) AND ADDRESS(ES)
Composites Branch (AFRL/RXCC)
Structural Materials Division
Air Force Research Laboratory, Materials and Manufacturing Directorate
Wright-Patterson Air Force Base, OH 45433-7750
Air Force Materiel Command, United States Air Force

8. PERFORMING ORGANIZATION REPORT NUMBER
AFRL-RX-WP-TP-2012-0377

9. SPONSORING/MONITORING AGENCY NAME(S) AND ADDRESS(ES)
Air Force Research Laboratory
Materials and Manufacturing Directorate
Wright-Patterson Air Force Base, OH 45433-7750
Air Force Materiel Command
United States Air Force

10. SPONSORING/MONITORING AGENCY ACRONYM(S)
AFRL/RXCC

11. SPONSORING/MONITORING AGENCY REPORT NUMBER(S)
AFRL-RX-WP-TP-2012-0377

12. DISTRIBUTION/AVAILABILITY STATEMENT
Approved for public release; distribution unlimited. Preprint to be submitted to Ceramics Engineering and Science Proceedings.

13. SUPPLEMENTARY NOTES
The U.S. Government is joint author of this work and has the right to use, modify, reproduce, release, perform, display, or disclose the work. PA Case Number and clearance date: 88ABW-2012-0777, 14 February 2012. This document contains color.

14. ABSTRACT
The strengths of Hi-NicalonTM-S SiC fibers were measured after oxidation in wet air between 700° and 1300°C. The oxidation and scale crystallization kinetics were also measured. Thicknesses of amorphous and crystalline scale were measured by TEM. Oxidation initially produces an amorphous scale that starts to crystallize to cristobalite and tridymite in 100 hours at 1000°C or in one hour at 1300°C. Crystallization kinetics for oxidation in wet air were slightly slower than those for dry air. The activation energy of 249 kJ/mol for parabolic oxidation to uncrystallized SiO2 scale in wet air was indistinguishable from that for dry air oxidation, but the pre-exponential factor was ~2x higher. SiC fiber strength changes with oxidation in dry and wet air were very similar. The fiber strength increased by approximately 10% for SiO2 scale thickness up to ~100 nm, and decreased for thicker scales. No significant strength degradation was observed for amorphous scales. All fibers with significantly degraded strength had crystallized or partially crystallized scales.

15. SUBJECT TERMS
SiC, Oxidation, Fibers

16. SECURITY CLASSIFICATION OF:			17. LIMITATION OF ABSTRACT:	NUMBER OF PAGES	19a. NAME OF RESPONSIBLE PERSON (Monitor)
a. REPORT	b. ABSTRACT	c. THIS PAGE			Randall Hay
Unclassified	Unclassified	Unclassified	SAR	10	19b. TELEPHONE NUMBER *(Include Area Code)* N/A

KINETICS OF PASSIVE OXIDATION OF HI-NICALON-S SiC FIBERS IN WET AIR: RELATIONSHIPS BETWEEN SiO_2 SCALE THICKNESS, CRYSTALLIZATION, AND FIBER STRENGTH

R. S. Hay, G. E. Fair
Air Force Research Laboratory
Materials and Manufacturing Directorate, WPAFB, OH

A. Hart, S. Potticary
U. Cincinnati, Cincinnati, OH

R. Bouffioux
New Mexico Tech. U., Socorro, NM

ABSTRACT

The strengths of Hi-Nicalon™-S SiC fibers were measured after oxidation in wet air between 700° and 1300°C. The oxidation and scale crystallization kinetics were also measured. Thicknesses of amorphous and crystalline scale were measured by TEM. Oxidation initially produces an amorphous scale that starts to crystallize to cristobalite and tridymite in 100 hours at 1000°C or in one hour at 1300°C. Crystallization kinetics for oxidation in wet air were slightly slower than those for dry air. The activation energy of 249 kJ/mol for parabolic oxidation to uncrystallized SiO_2 scale in wet air was indistinguishable from that for dry air oxidation, but the pre-exponential factor was ~2x higher. SiC fiber strength changes with oxidation in dry and wet air were very similar. The fiber strength increased by approximately 10% for SiO_2 scale thickness up to ~100 nm, and decreased for thicker scales. No significant strength degradation was observed for amorphous scales. All fibers with significantly degraded strength had crystallized or partially crystallized scales.

INTRODUCTION

SiC fiber strength is affected by oxidation. Fiber strength defines the maximum attainable CMC strength.[1] Oxidation is affected by fiber impurities, particularly alkali and alkali earths, that increase oxidation rates, reduce scale viscosity, and lower temperatures for scale crystallization.[2-3] Moisture has similar effects.[4-9] Some work suggests that oxidation of SiC fibers reduces their strength.[10-17] However, recent work has shown that thin silica scales (< 100 nm) actually increase SiC fiber strength,[18-21] as might be expected from surface flaw healing and residual compressive stress in the scales. Ambiguous effects of SiC oxidation on strength have also been observed for bulk material.[22-23]

Preliminary data and analysis for the oxidation kinetics, scale crystallization kinetics, and strength of Hi-Nicalon™-S SiC (β-SiC) fiber oxidized in wet air are presented. This paper builds on a thorough description and analysis of Hi-Nicalon™-S SiC fiber oxidation and scale crystallization kinetics in dry air.[20-21] Hi-Nicalon™-S fiber was chosen because it has near-stoichiometric SiC composition (~1 at% oxygen and ~2 at% carbon),[24] and the smoothest surface of currently available SiC fibers.[25] The fiber properties are described in several publications.[11, 24, 26-30]

EXPERIMENTS

Hi-Nicalon™-S fibers have a PVA (polyvinyl alcohol) sizing. To avoid contamination of the fiber surface by sizing impurities, the sizing was removed by two sequential dissolutions in boiling distilled deionized water in a Pyrex glass beaker for one hour.[20-21] The desized fibers were oxidized in flowing wet air by bubbling dry air through distilled water at room temperature (24°C). Water saturation at this temperature yields a water/air molar ratio of 0.03. Fibers were oxidized in an alumina muffle tube furnace with an alumina boat dedicated to these experiments. Both the muffle tube and boat were baked-out at 1540°C for 4 hours in laboratory air prior to use. These bake-outs have been shown to be necessary to prevent contamination by alumina impurities.[31] Fiber oxidation was done at 700 to 1300°C for times up to 100 hours. A total of 20 different heat-treatments were done (Table I). Heat-up and cool-down rates of 10°C/minute were used.

The strengths of the oxidized fibers were measured by tensile testing at least 30 filaments, using published methods.[32] The average and Weibull characteristic value for failure stress were

calculated, along with the Weibull modulus. Strengths were calculated using both the original ($\mathbf{r_i}$) and final SiC radius after oxidation ($\mathbf{r_f}$) (Fig. 1). The average fiber diameter measured by optical microscopy and SEM was 12.1 μm.

The uniformity SiO_2 scale uniformity was characterized using reflected light interference fringes observed by optical microscopy. Cross-sectional TEM specimens were prepared from oxidized fibers by published methods.[33-34] TEM sections were ion-milled at 5 kV and examined using a 200 kV Phillips LaB_6-filament TEM and a 300 kV FEI Titan TEM. SiO_2 oxidation product thickness (**x**) and cracking, fraction of crystallized scale (***f***), and microstructures of the SiO_2 scale were characterized for a minimum of five filaments, and in many cases more than ten. The crystallized SiO_2 phase (tridymite or cristobalite) was identified from selected area electron diffraction patterns in some scales.

***Fig. 1**. Diagram showing initial (r_i) and final (r_f) SiC thickness after oxidation and SiO_2 thickness **x**.*

RESULTS AND DISCUSSION

Results for twenty wet oxidation experiments are shown in Table I. All reported strengths are calculated from the final SiC radius present after oxidation.

#	# of Obs.	T (°C)	t (hrs)	x (nm) *amorphous*	x (nm) *crystalline*	*f*	Strength (GPa)	Weib. Char. (GPa)	Weibull Modulus	Comments
1	29	700	100	17.7 ± 5.7	—	0	2.64	2.93	7.71	
2	38	800	1	7.2 ± 1.6	—	0	2.98	3.15	5.89	
3	22	800	10	20.1 ± 11.3	—	0	2.80	3.13	2.96	1 outlier – 0.66 GPa
4	43	800	100	74.1 ± 11.1	—	0	3.05	3.18	4.90	
5	23	900	1	15.9 ± 4.3	—	0	2.77	2.86	5.64	
6	45	900	10	72.0 ± 5.6	—	0	2.73	2.87	6.98	
7	15	900	100	216. ± 8.	—	0	2.77	3.17	4.11	
8	30	1000	1	66.0 ± 5.4	—	0.036	3.14	3.25	6.67	
9	66	1000	10	198. ± 10.	—	0.04	3.15	3.28	6.36	
10	23	1000	30	333. ± 15.	—	0.043	2.82	2.93	7.47	
11	30	1000	100	859. ± 29.	841..± 62.	0.15	2.44	2.83	2.70	
12	15	1050	100	—	1470. ± 110.	1	<1	<1	—	6 Tridymite, 1 Cristobalite
13	39	1100	1	167. ± 7.	—	0	2.40	2.77	2.46	
14	22	1100	3	214. ± 17.	—	0	2.82	3.14	5.55	
15	75	1100	10	652. ± 24.	623. ± 53.	0.44	2.14	2.37	3.05	11 Tridymite, 4 Cristobalite
16	5	1100	100	—	1590. ± 79.	1	<1	<1	—	1 Tridymite
17	6	1200	1	274. ± 16.	257. ± 41.	0.2	2.38	2.71	4.06	1 Tridymite
18	5	1200	10	—	790.±90.	1	2.07	2.08	4.68	2 Cristobalite
19	11	1200	100	—	2390. ± 200.	1	<1	<1	—	1 Tridymite
20	13	1300	1	601.±49.	456. ± 17.	0.77	2.55	2.56	4.93	1 Tridymite, 1 Cristobalite

***Table I**. Hi-Nicalon^{1M}-S wet-air oxidation experiments. **f** is the fraction of scale that is crystallized.*

Fiber Strength

The relationship between oxide scale thickness (**x**) and the Weibull characteristic strength of the fibers is shown in figure 2. As-received fibers had average strengths of 2.85 GPa and Weibull characteristic strengths of 3.0 GPa; this is plotted at x = 1 nm on the logarithmic scale thickness axis. Tensile strengths could not be reliably measured for some fibers with thick, crystallized scales. Extensive experience with filament tensile testing suggests that these fibers have tensile strengths less than 1 GPa, as indicated in Table I and figure 2. Fiber strengths in figure 2 are shown as a function of scale thickness after oxidation at various times at 700 - 1300°C for both dry and wet air oxidation. Dry air is denoted by discs and wet air by circles. Amorphous scales are red, fully crystallized scales are purple, and partially crystallized scales have colors between red and purple, with a hue proportional to the fraction of scale crystallized (***f***) in Table I. The strengths are plotted for the final SiC fiber radius ($\mathbf{r_f}$) after oxidation, which can be calculated from the original fiber radius ($\mathbf{r_i}$) and the oxide scale thickness (**x**) from:

$$\mathbf{r_f} = [\mathbf{x}^2 (\Omega_{SiC}{}^2/\Omega_{SiO2}{}^2 - \Omega_{SiC}/\Omega_{SiO2}) + \mathbf{r_i}^2]^{1/2} - (\Omega_{SiC}/\Omega_{SiO2})\mathbf{x} \quad [1]$$

where Ω_{SiC} and Ω_{SiO2} are the molar volumes for SiC and SiO_2, respectively. The load carried by the SiO_2 scale, which has a modulus less than 1/5 that of SiC, is insignificant and beneath measurement error.

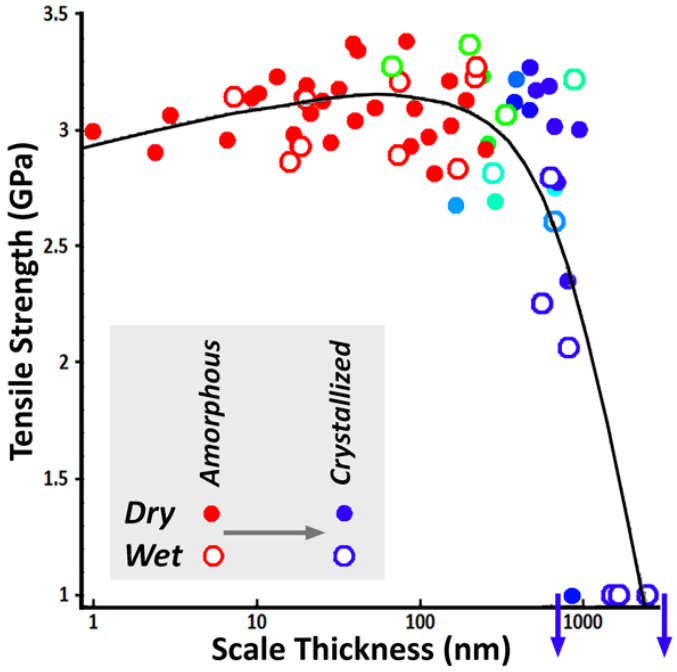

Fig. 2 *Weibull characteristic fiber strength vs. oxide scale thickness.*

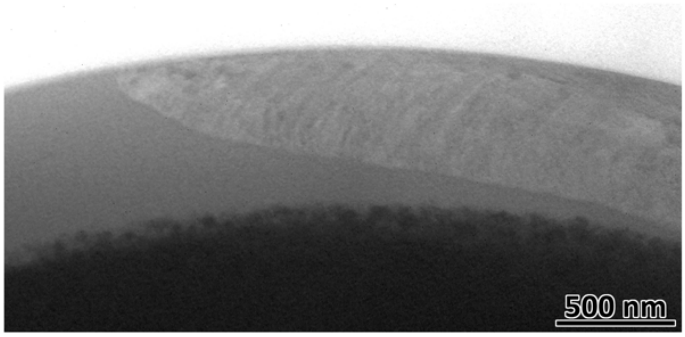

Fig. 3 *TEM micrograph of SiO_2 crystallization after oxidation in wet air for 10 h at 1100°C.*

Fiber strength increased about 10% for thin oxide scales, with a weakly defined maximum near SiO_2 thicknesses of ~50 – 100 nm. As observed for dry air oxidation,[21] there was no relationship between oxidation temperature and fiber strength; scales of similar thickness that formed in a short time at high temperature or a long time at low temperature had similar effects on fiber strength. No significant strength degradation was observed for fibers with amorphous scales. All fibers with Weibull characteristic strengths <2.75 GPa had crystallized or partially crystallized scales (Fig. 2). However, there were some fibers with crystallized or partially crystallized scales that were not significantly degraded in strength. Detailed analysis of Weibull parameters as well as a discussion of possible strengthening and degradation mechanisms will be done in future papers covering dry air, wet air, and active oxidation experiments.

Crystallization

As in dry air oxidation,[20-21] crystallization always nucleated at the scale surface, and growth was comparatively rapid parallel to the surface than through thickness (Fig. 3). EDS measurements for dry air oxidation suggest some carbon incorporated in the amorphous scale was later rejected during crystallization.[20-21] We have not yet checked this for wet-air oxidation.

SiO_2 crystallized to cristobalite and various tridymite polymorphs at 1000° - 1300°C (Fig. 4, Table I). Tridymite dominated. This was also observed in dry air oxidation.[20-21] The relative abundance of cristobalite increased at higher temperatures (Table I), as observed in other studies.[35-37] Crystalline silica scales were thinner than corresponding amorphous scales, as observed previously,[38] and the thicknesses of crystalline scales were more variable (Table I). Nucleation was not synchronous, so such variation could be caused by variation in the amount of time spent in amorphous and crystalline states.

Crystallized SiO_2 scales often cracked (Fig. 4). Debond cracks between SiO_2 scale and SiC were also common. Cracked crystalline scales were previously observed Hi-Nicalon™ and Hi-Nicalon™-S,[20-21] and were suggested to cause lower fiber strengths.[10, 39] Unlike amorphous SiO_2, cristobalite and tridymite have larger coefficients of thermal expansion than SiC, particularly near room temperature.[40-41] Cracks are assumed to form from thermal stress during cooling, and from volume contraction during tridymite phase transformations and the $\alpha \rightarrow \beta$ cristobalite phase transformation.

Thick crystalline scales had wide aperture cracks parallel with the fiber axis that clearly formed during oxidation (Fig. 4). They are inferred to be caused by tensile hoop growth stress that develops during oxidation of cylindrical substrates, which in turn is caused by the 2.2× volume expansion for SiC oxidation.[42-48] When these cracks form the scale is no longer passivating; they are a short-circuit

path for O_2 ingress and SiC oxidation rates are increased underneath them.[45] Other cracks, generally with narrower apertures, formed perpendicular to the fiber axis, as observed for dry air oxidation.[20-21]

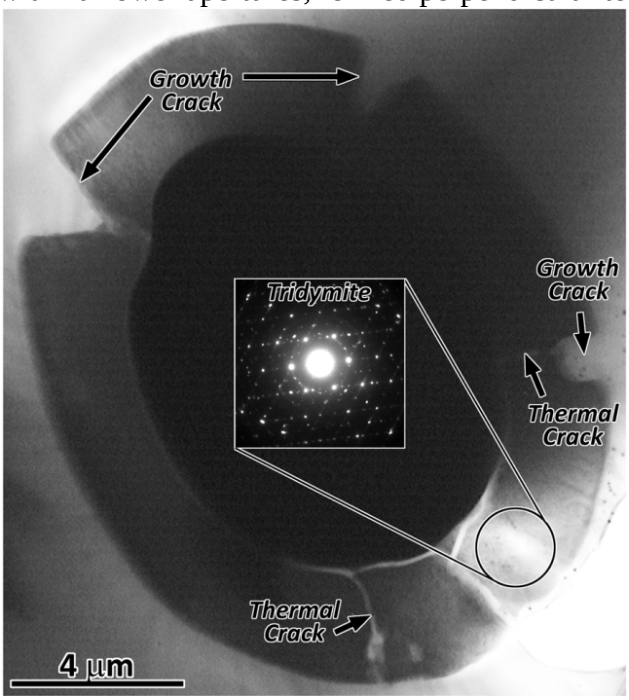

Fig. 4 *TEM micrograph of SiO_2 crystallization after oxidation in wet air for 100 h at 1200°C. Thermal and growth cracks are identified. An inset shows a selected area electron diffraction pattern for tridymite.*

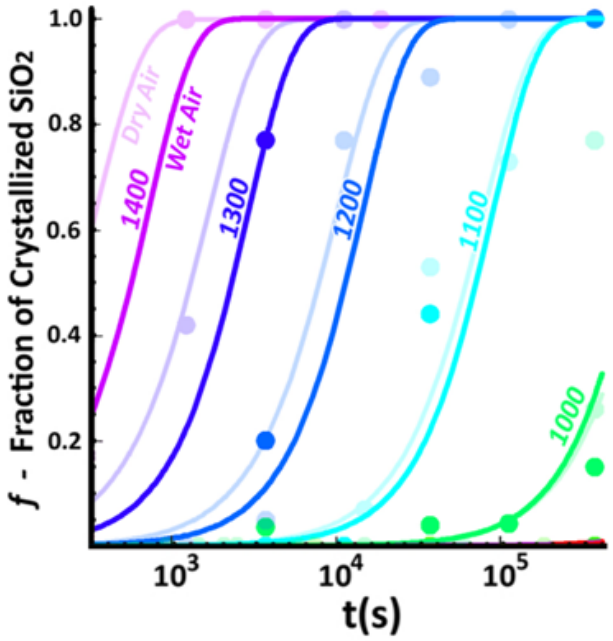

Fig. 5 *Avrami plot of crystallization kinetic data from Table I. Wet air data and parameter fit is in bold; dry air data and parameter fit from earlier work is faded.*

Kolmogorov-Johnson-Mehl-Avrami (KJMA) analysis was used for silica crystallization kinetics:[49-50]

$$\boldsymbol{f} = 1 - \exp[-\mathbf{K}\mathbf{t}^{\mathbf{n}}] \quad [2]$$

$$\mathbf{K} = \mathbf{K_o}\exp[-\mathbf{Q}/\mathrm{R}\mathbf{T}] \quad [3]$$

where ***f*** is the fraction crystallized (Table I), **K** is a rate constant, **t** is time, **n** is a the time growth exponent, $\mathbf{K_o}$ is a pre-exponential factor and **Q** an activation energy for growth, and R**T** has the usual meaning in an Arrhenius expression. A parameter best fit for all **t**, **T**, and ***f*** yields:

$$\mathbf{Q} = 487\ \mathrm{kJ/mol} \quad [4a]$$

$$\mathbf{K_o} = 5 \times 10^{10} \quad [4b]$$

$$\mathbf{n} = 1.6 \quad [4c]$$

The parameter fit is shown in figure 5, along with the data and fit found previously for dry air oxidation.[20-21] The wet air activation energy **Q** is slightly lower than that found for dry air (514 kJ/mol), $\mathbf{K_o}$ is 40× lower, and the time growth exponents (**n**) are similar.[20-21] Crystallization kinetics were slightly slower in wet air than in dry air, particularly at high temperatures (Fig. 5). A growth exponent **n** of ~1.5 is diagnostic of three-dimensional growth from site-saturated nucleation.[50]

Oxidation Kinetics – Amorphous Scale

No cracks were observed in amorphous scales, even in scales nearly a micron thick. Thick scales were uniform; thin scales had higher relative variability in thickness (Table I). This was also observed for dry air oxidation.[20-21]

Passive oxidation kinetics for SiC in wet air were analyzed using Deal-Grove kinetics for flat plates, with diffusion of molecular O_2 through SiO_2 as the rate limiting step in the parabolic regime.[9, 51] Flat plate geometry was shown to be accurate for scale thicknesses < 1 μm on a 6.5 μm radius fiber.[20-21] A more detailed description of the analysis methods that includes corrections for scale formed during heat-up and cool-down is given elsewhere.[20-21]

The thickness of the SiO_2 scale (**x**) described by Deal-Grove kinetics for the flat plate geometry is:

$$d\mathbf{x}/d\mathbf{t} = \mathbf{B}/(\mathbf{A} + 2\mathbf{x}) \quad [5]$$

$$\mathbf{A} = \mathbf{A_o} \exp[-\mathbf{Q_a}/\mathbf{RT}] \quad [6]$$
$$\mathbf{B} = \mathbf{B_o} \exp[-\mathbf{Q_b}/\mathbf{RT}] \quad [7]$$

where $\mathbf{A_o}$ and $\mathbf{B_o}$ are constants and $\mathbf{Q_a}$ and $\mathbf{Q_b}$ are activation energies. **B** is the parabolic rate constant and **B**/**A** is the linear rate constant. For an initial SiO_2 thickness of $\mathbf{x_i}$, the solution to [5] is:

$$\mathbf{x} = \tfrac{1}{2}\mathbf{A}\{[1+ (\mathbf{t} + \boldsymbol{\tau})/(\mathbf{A}^2/4\mathbf{B})]^{1/2} - 1\} \quad [8]$$
$$\boldsymbol{\tau} = (\mathbf{x_i}^2 + \mathbf{A}\mathbf{x_i})/\mathbf{B} \quad [9]$$

where $\boldsymbol{\tau}$ is a time shift that corrects for presence of an initial oxide layer. For long times, [8] becomes the simple expression for parabolic oxidation kinetics:

$$\mathbf{x}^2 = \mathbf{B}\,\mathbf{t} \quad [10]$$

The best fit for "Deal-Grove" parameters for oxidation kinetics for amorphous SiO_2 scale formation for Hi-Nicalon^{TM}-S fiber in wet air are:

$$\mathbf{A_o} = 8.1 \times 10^{-4}\ \text{m} \quad [11a]$$
$$\mathbf{Q_a} = 108\ \text{kJ/mol} \quad [11b]$$
$$\mathbf{B_o} = 2.2 \times 10^{-8}\ \text{m}^2/\text{s} \quad [11c]$$
$$\mathbf{Q_b}\ (\text{parabolic}) = 249\ \text{kJ/mol} \quad [11d]$$
$$\mathbf{Q_{b/a}}\ (\text{linear}) = 141\ \text{kJ/mol} \quad [11e]$$

As found for dry air oxidation, the fit had strong convergence to the $\mathbf{Q_b}$ value, but was less sensitive to the other parameters, particularly $\mathbf{Q_a}$ and $\mathbf{A_o}$. Data and the parameter fit are plotted in figure 6, along with predicted values for various crystallization fractions (***f***) from [2-4]. $\mathbf{Q_a}$ and $\mathbf{Q_b}$ values for wet air oxidation were almost identical to those for dry air oxidation, but the pre-exponential factors $\mathbf{A_o}$ and $\mathbf{B_o}$ were ~2× higher. The 2× factor increase with little change in temperature dependence for P_{H2O} of ~ 0.03 is roughly consistent with other observations of oxidation rate increases in water environments.[52-53] More detailed analysis and discussion will be presented in publications building on this preliminary study.

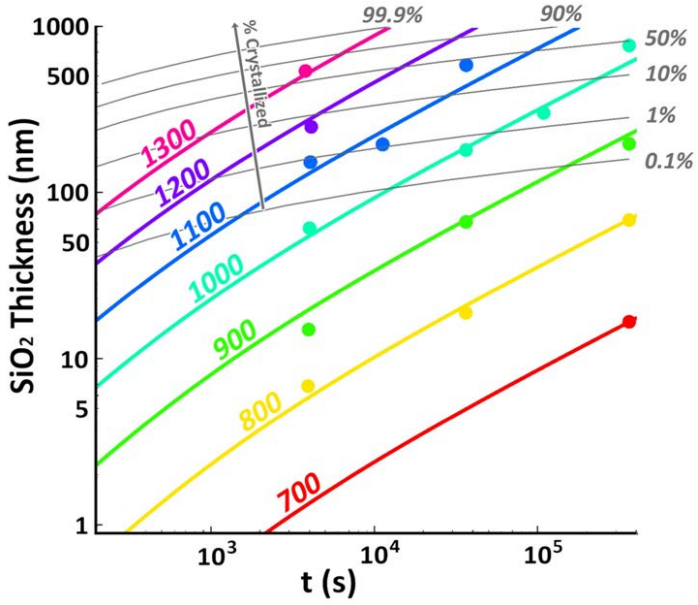

Fig. 6 *Deal-Grove oxidation kinetics parameter fits [5-11] to data in Table I. Data and fit are for amorphous SiO_2 scale growth in wet air for Hi-Nicalon^{TM}-S SiC fiber. Avrami crystallization kinetics predictions for various f values [2-4] are superimposed.*

SUMMARY AND CONCLUSIONS

The Deal-Grove oxidation kinetics for amorphous SiO_2 scales, Avrami scale crystallization kinetics, and tensile strength of Hi-Nicalon^{TM}-S SiC fiber were measured after oxidation in wet air at 700° to 1300°C for up to 100 hours. The results are generally similar to those previously found for oxidation in dry air. Activation energies for both oxidation and crystallization rates were similar in dry and wet air. However, wet air oxidation had approximately a 2× increase in the pre-exponential factors $\mathbf{A_o}$ and $\mathbf{B_o}$ for linear and parabolic oxidation, respectively, and a decrease in scale crystallization rate at the higher temperatures in comparison with dry air parameters. As observed for dry air oxidation, the fiber strength increased by approximately 10% for SiO_2 scale thickness up to ~100 nm, and decreased for thicker scales. No significant strength degradation was observed for amorphous scales. All fibers with significantly

degraded strength had crystallized or partially crystallized scales. Scale crystallization typically began at thicknesses greater than 100 nm. Amorphous scales were uncracked. Crystalline scales were cracked from thermal stress, polymorphic phase transformations, and tensile hoop growth stress. These cracks are inferred to be responsible for lower fiber strength. Future work will try to establish quantitative relationships between fiber strength, oxidation kinetics, crystallization kinetics, and scale residual stress.

REFERENCES

1. Curtin WA, Ahn BK, Takeda N. Modeling Brittle and Tough Stress-Strain Behavior in Unidirectional Ceramic Matrix Composites. Acta mater. 1998;46(10):3409-20.
2. Doremus RH. Viscosity of Silica. J. Appl. Phys. 2002;92(12):7619-29.
3. Pezzotti G, Painter GS. Mechanisms of Dopant-Induced Changes in Intergranular SiO_2 Viscosity in Polycrystalline Silicon Nitride. J. Am. Ceram. Soc. 2002;85(1):91-96.
4. Akashi T, Kasajima M, Kiyono H, Shimada S. SIMS Study of SiC Single Crystal Oxidized in Atmosphere Containg Isotopic Water Vapor. J. Ceram. Soc. Japan 2008;116(9):960-64.
5. Opila EJ, Hann RE. Paralinear Oxidation of CVD SiC in Water Vapor. J. Am. Ceram. Soc. 1997;80(1):197-205.
6. Opila EJ. Oxidation Kinetics of Chemically Vapor-Deposited Silicon Carbide in Wet Oxygen. J. Am. Ceram. Soc. 1994;77(3):730-36.
7. Narushima T, Goto T, Hirai T. High-Temperature Passive Oxidation of Chemically Vapor deposited Silicon Carbide. J. Am. Ceram. Soc. 1989;72(8):1386-90.
8. Maeda M, Nakamura K, Ohkubo T. Oxidation of Silicon Carbide in a Wet Atmosphere. J. Mater. Sci. 1988;23:3933-38.
9. Presser V, Nickel KG. Silica on Silicon Carbide. Crit. Rev. Solid State Mater. Sci. 2008;33:1-99.
10. Takeda M, Urano A, Sakamoto J, Imai Y. Microstructure and Oxidation Behavior of Silicon Carbide Fibers Derived from Polycarbosilane. J. Am. Ceram. Soc. 2000;83(5):1171-76.
11. Shimoo T, Takeuchi H, Okamura K. Oxidation Kinetics and Mechanical Property of Stoichiometric SiC Fibers (Hi-Nicalon-S). J. Ceram. Soc. Japan 2000;108(1264):1096-102.
12. Kim H-E, Moorhead AJ. Strength of Nicalon Silicon Carbide Fibers Exposed to High-Temperature Gaseous Environments. J. Am. Ceram. Soc. 1991;74(3):666-69.
13. Brennan JJ. Interfacial Characterization of a Slurry-Cast Melt-Infiltrated SiC/SiC Ceramic-Matrix Composite. Acta mater. 2000;48(18/19):4619-28.
14. Gauthier W, Pailler F, Lamon J, Pailler R. Oxidation of Silicon Carbide Fibers During Static Fatigue in Air at Intermediate Temperatures. J. Am. Ceram. Soc. 2009;92(9):2067-73.
15. Gogotsi Y, Yoshimura M. Oxidation and Properties Degradation of SiC Fibres Below 850 C. J. Mater. Sci. Lett. 1994;13:680-83.
16. Lara-Curzio E. Stress-Rupture of Nicalon/SiC Continuous Fiber Ceramic Composites in Air at 950 C. J. Am. Ceram. Soc. 1997;80(12):3268-72.
17. Lara-Curzio E. Oxidation Induced Stress-Rupture of Fiber Bundles. J. Eng. Mater. Tech 1998;120:105-09.
18. Hay RS, Fair GE, Urban E, Morrow J, Somerson J, Wilson M. Oxidation Kinetics and Strength Versus Scale Thickness for Hi-Nicalon^{TM}-S Fiber. In: Singh Z, Zhou, and Singh, editor. Ceramic Transactions; 2010.
19. Mogilevsky P, Boakye EE, Hay RS, Kerans RJ. Monazite Coatings on SiC Fibers II: Oxidation Protection. J. Am. Ceram. Soc. 2006;89(11):3481-90.
20. Hay RS, Fair GE, Bouffioux R, Urban E, Morrow J, Somerson J, et al. Hi-Nicalon^{TM}-S SiC Fiber Oxidation and Scale Crystallization Kinetics. J. Am. Ceram. Soc. 2011;94(11):3983-91.
21. Hay RS, Fair GE, Bouffioux R, Urban E, Morrow J, Hart A, et al. Relationships between Fiber Strength, Passive oxidation and Scale Crystallization Kinetics of Hi-Nicalon^{TM}-S SiC Fibers. Ceram. Eng. Sci. Proc. 2011;32(2):39-54.
22. Easler TE, Bradt RC, Tressler RE. Strength Distributions of SiC Ceramics After Oxidation and Oxidation Under Load. J. Am. Ceram. Soc. 1981;64(12):731-34.
23. Badini C, Fino P, Ortona A, Amelio C. High Temperature Oxidation of Multilayered SiC Processed by Tape Casting and Sintering. J. Eur. Ceram. Soc. 2002;22:2017-79.

24. Dong SM, Chollon G, Labrugere C, Lahaye M, Guette A, Bruneel JL, et al. Characterization of Nearly Stoichiometric SiC Fibres. J. Mater. Sci. 2001;36:2371-81.
25. Hinoki T, Snead LL, Lara-Curzio E, Park J, Kohyama A. Effect of Fiber/Matrix Interfacial Properties on Mechanical Properties of Unidirectional Crystalline Silicon Carbide Composites. Ceram. Eng. Sci. Proc. 2002;23(3):511-18.
26. Sauder C, Lamon J. Tensile Creep Behavior of SiC-Based Fibers With a Low Oxygen Content. J. Am. Ceram. Soc. 2007;90(4):1146-56.
27. Bunsell AR, Piant A. A Review of the Development of Three Generations of Small Diameter Silicon Carbide Fibres. J. Mater. Sci. 2006;41:823-39.
28. Ishikawa T. Advances in Inorganic Fibers. Adv. Polym. Sci. 2005;178:109-44.
29. Sha JJ, Nozawa T, Park JS, Katoh Y, Kohyaman A. Effect of Heat-Treatment on the Tensile Strength and Creep Resistance of Advanced SiC Fibers. J. Nucl. Mater. 2004;329-333:592-96.
30. Tanaka T, Shibayama S, Takeda M, Yokoyama A. Recent Progress of Hi-Nicalon Type S Development. Ceram. Eng. Sci. Proc. 2003;24(4):217-23.
31. Opila E. Influence of Alumina Reaction Tube Impurities on the Oxidation of Chemically-Vapor-Deposited Silicon Carbide. J. Am. Ceram. Soc. 1995;78(4):1107-10.
32. Petry MD, Mah T, Kerans RJ. Validity of Using Average Diameter for Determination of Tensile Strength and Weibull Modulus of Ceramic Filaments. J. Am. Ceram. Soc. 1997;80(10):2741-44.
33. Hay RS, Welch JR, Cinibulk MK. TEM Specimen Preparation and Characterization of Ceramic Coatings on Fiber Tows. Thin Solid Films 1997;308-309:389-92.
34. Cinibulk MK, Welch JR, Hay RS. Preparation of Thin Sections of Coated Fibers for Characterization by Transmission Electron Microscopy. J. Am. Ceram. Soc. 1996;79(9):2481-84.
35. Guinel MJF, Norton MG. Oxidation of Silicon Carbide and the Formation of Silica Polymorphs. J. Mater. Res. 2006;21(10):2550-63.
36. Horvath E, Zsiros G, Toth AL, Sajo I, Arato P, Pfeifer J. Microstructural Characterization of the Oxide Scale on Nitride Bonded SiC-Ceramics. Ceramics Int. 2008;34:151-55.
37. Schneider H, Flörke OW. High-temperature transformation of tridymite single crystals to cristobalite*. Zeitschrift für Kristallographie 1986;175(3-4):165-76.
38. Presser V, Loges A, Hemberger Y, Nickel KG. Microstructural Evolution of Silica on Single-Crystal Silicon Carbide. Part I: Devitrification and Oxidation Rates. J. Am. Ceram. Soc. 2009;92(3):724-31.
39. Shimoo T, Hayatsu T, Takeda M, Ichikawa H, Seguchi T, Okamura K. Mechanism of Oxidation of Low-Oxygen SiC Fiber Prepared by Electron Radiation Curing Method. J. Ceram. Soc. Japan 1994;102(7):617-22.
40. Sosman RB. Mechanical and Thermal Properties of the Various Forms of Silica. In: Washburn E, editor. International Critical Tables of Numerical Data, Physics, Chemistry and Technology (Volume 3): McGraw-Hill Book Company, Inc.; 1928. p. 19-25.
41. Mao H, Sundman B, Wang Z, Saxena SK. Volumetric Properties and Phase Relations of Silica - Thermodynamic Assessment. J. Alloys and Compounds 2001;327:253-62.
42. Delph TJ. Intrinsic strain in SiO_2 thin films. J. Appl. Phys. 1998;83(2):786-92.
43. Kao D-B, McVittie JP, Nix WD, Saraswat KC. Two-Dimensional Thermal Oxidation of Silicon - II. Modeling Stress Effects in Wet Oxides. IEEE Trans. Electron. Dev. 1988;35(1):25-37.
44. Rafferty CS, Borucki L, Dutton RW. Plastic Flow During the Thermal Oxidation of Silicon. Appl. Phys. Lett. 1989;54(16):1516-18.
45. Chollon G, Pallier R, Naslain R, Laanani F, Monthioux M, Olry P. Thermal Stability of a PCS-Derived SiC Fibre with a Low Oxygen Content (Hi-Nicalon). J. Mater. Sci. 1997;32:327-47.
46. Hsueh CH, Evans AG. Oxidation Induced Stresses and Some Effects on the Behavior of Oxide Films. J. Appl. Phys. 1983;54(11):6672-86.
47. Brown DK, Hu SM, Morrissey JM. Flaws in Sidewall Oxides Grown on Polysilicon Gate. J. Electrochem. Soc. 1982;129(5):1084-89.
48. Hay RS. Growth Stress in SiO_2 during Oxidation of SiC Fibers. J. Appl. Phys. submitted.

49. Liu F, Sommer F, Mittemeijer EJ. Analysis of the Kinetics of Phase Transformations; Roles of Nucleation Index and Temperature Dependent Site Saturation, and Recipes for the Extraction of Kinetic Parameters. J. Mater. Sci. 2007;42:573-87.
50. Liu F, Sommer F, Bos C, Mittemeijer EJ. Analysis of Solid State Phase Transformation Kinetics: Models and Recipes. Int. Mater. Rev. 2007;52(4):193-212.
51. Deal BE, Grove AS. General Relationships for the Thermal Oxidation of Silicon. J. Appl. Phys. 1965;36(12):3770-78.
52. Opila EJ. Variation of the Oxidation Rate of Silicon Carbide with Water Vapor Pressure. J. Am. Ceram. Soc. 1999;82(3):625-36.
53. Yoshimura M, Kase J, Somiya S. Oxidation of SiC Powder by High-Temperature, High-Pressure H_2O. J. Mater. Res. 1986;1(1):100-03.